Supplementary Information (SI) for Materials Horizons.

Supporting Information

Room-Temperature Synthesized Triple Cation Green Perovskite Quantum Dots for Optoelectronic Applications

Jean-Sébastien Bénas[a], Fang-Cheng Liang[a], Yu-Hang Huang[a], Fu-Chieh Liu[a], Chun-Hsine Ou[a], Ryosuke Oikawa[b], Ryota Kobayashi[b], Shoki Mizoguchi[b], Yuna Igarashi[b], Takayuki Chiba[b,*], Junji Kido[b,*] and Chi-Ching Kuo[a,c,*]

[a] Institute of Organic and Polymeric Materials, National Taipei University of Technology, Taipei 10608, Taiwan

[b] Graduate School of Organic Materials Science, Frontier Center for Organic Materials, Yamagata University, 4-3-16 Jonan, Yonezawa 992-8510, Japan

[c] Advanced Research Center for Green Materials Science and Technology, National Taiwan University, Taipei 10617, Taiwan

*Author to whom all correspondence should be addressed

Tel.: 886-2-27712171*2407; Fax: 886-2-27317174

Correspondence to: Prof. C.-C. Kuo (E-mail: kuocc@mail.ntut.edu.tw)

Prof. J. Kido (E-mail: kid@yz.yamagata-u.ac.jp)

Prof. T. Chiba (E-mail: T-chiba@yz.yamagata-u.ac.jp)

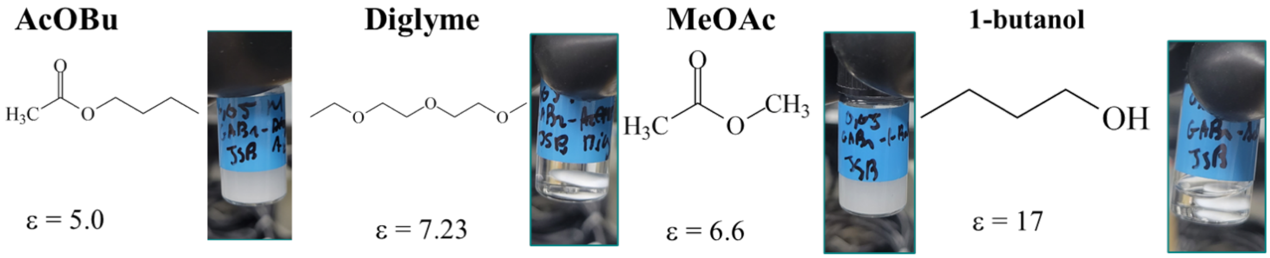

Figure S1. Solubility test of GABr. Each solvent structure is represented with their dielectric constant. On the right side, for each solvent, is shown the result of the dissolution process after one hour of stirring.

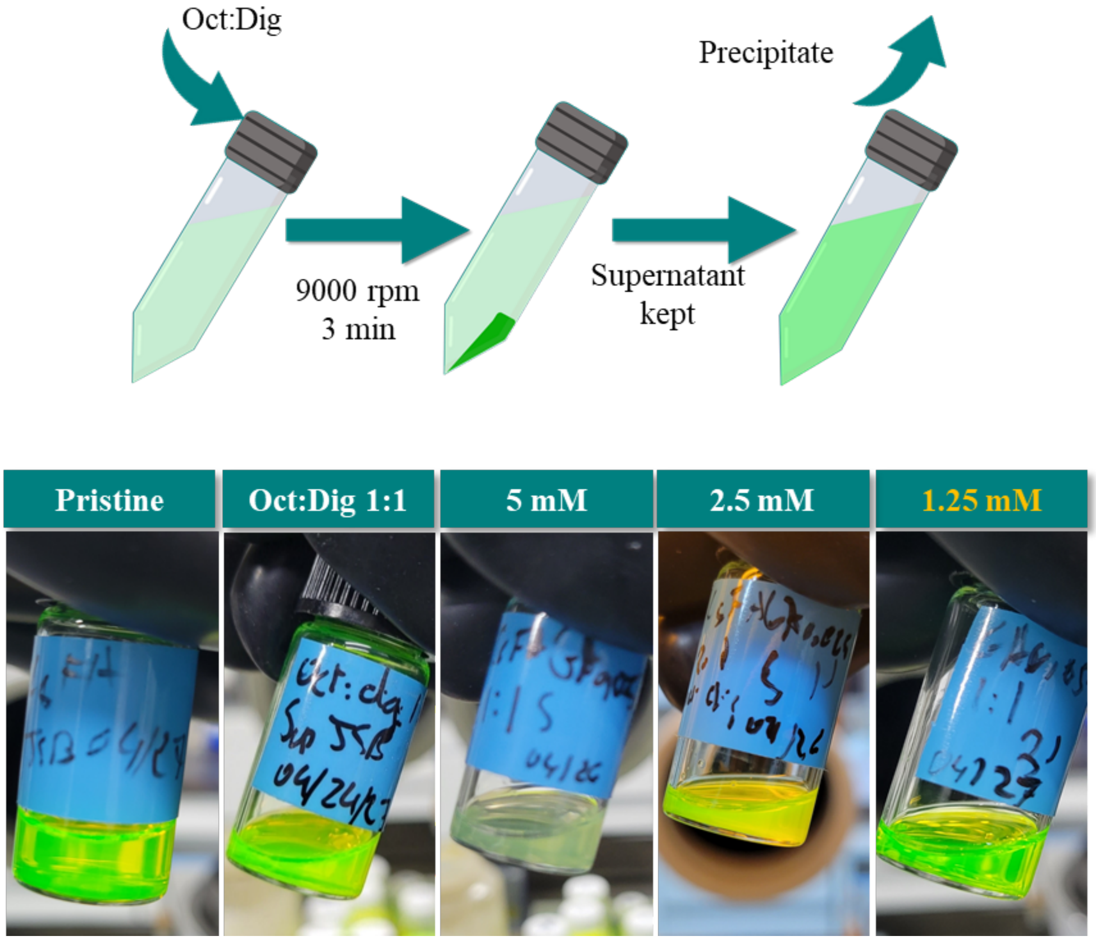

Figure S2. The impact of diglyme onto CsFAPbBr$_3$ PQDs colloidal stability is shown. The second picture from the left shows the PQDs ink after diglyme washing process. Further three photograph highly the impact of GABr:Dig washing process as the GABr molar ratio is decreased.

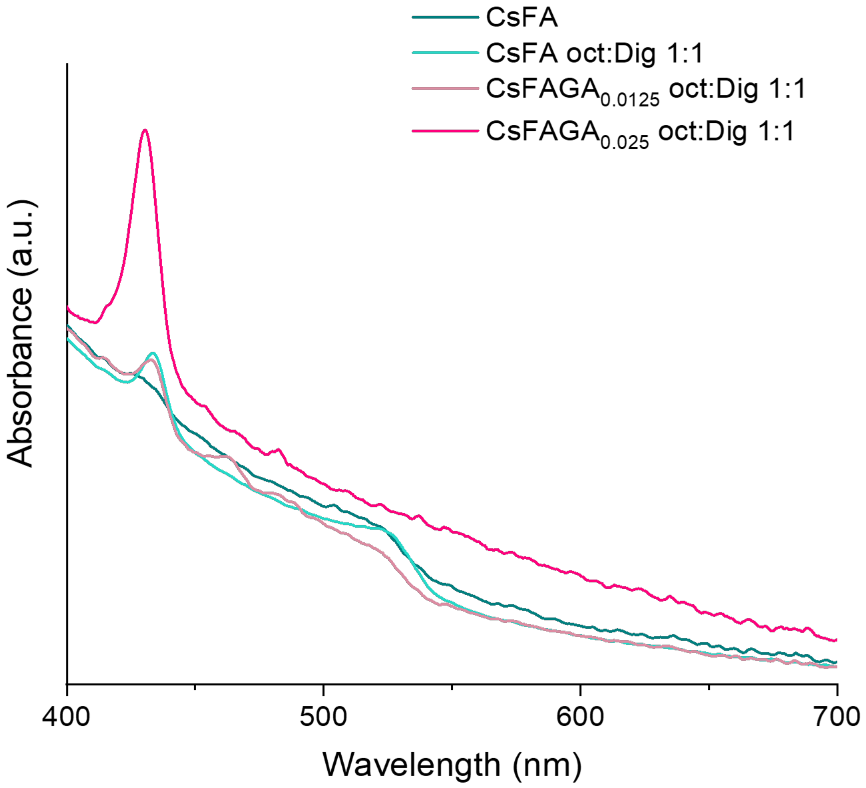

Figure S3: UV absorption of post-synthesis GA-doped triple cation PQDs.

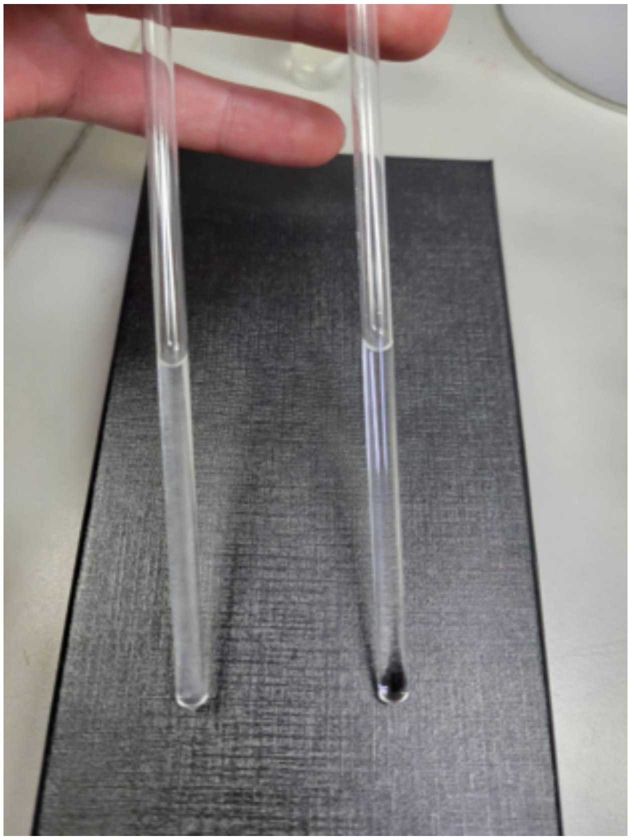

Figure S4: Photograph of GA-FA dispersed in Diglyme solvent (left tube) and GA dispersed in diglyme (right tube) for NMR observation. Upon redispersion in $CdCl_3$, GA has reprecipitated.

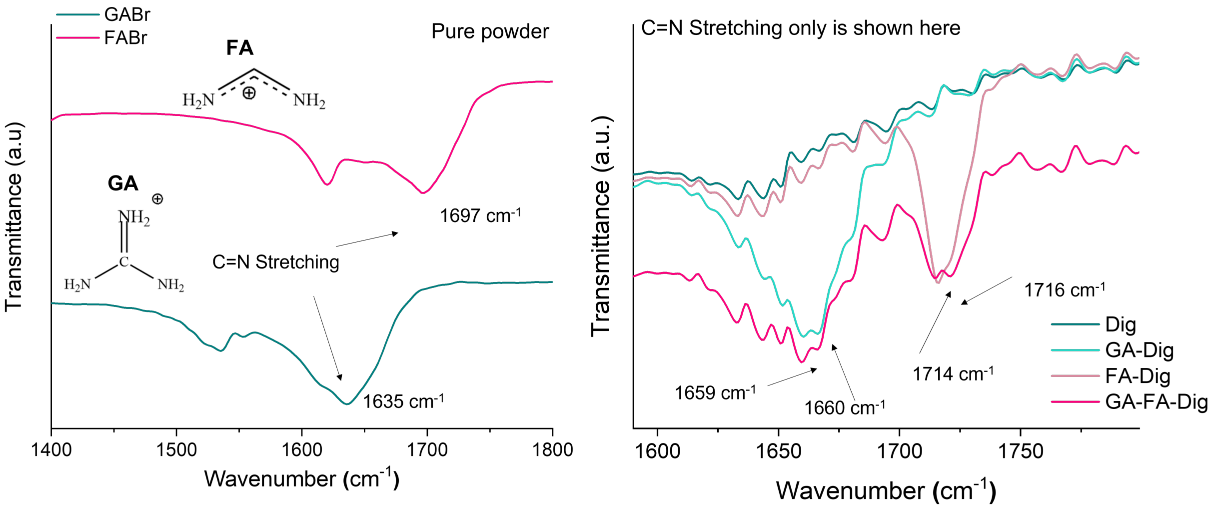

Figure S5: FTIR of GABr and FABr powder centered on the -C=N- stretching (left) and when incorporated into diglyme solvent (right).

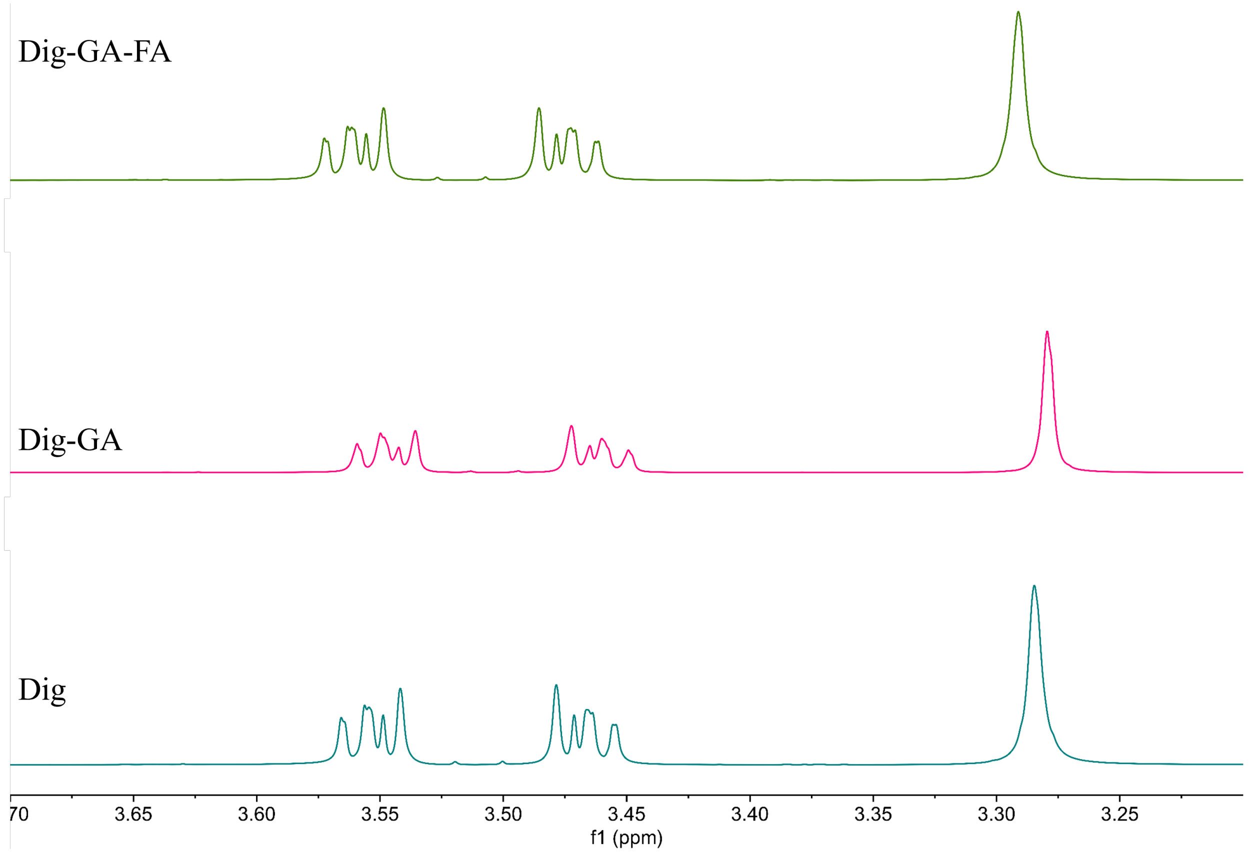

Figure S6: NMR spectra of Diglyme, GA dispersed into Diglyme and GA-FA mixture dispersed into Diglyme and centered onto Diglyme methylene and methyl group chemical shift.

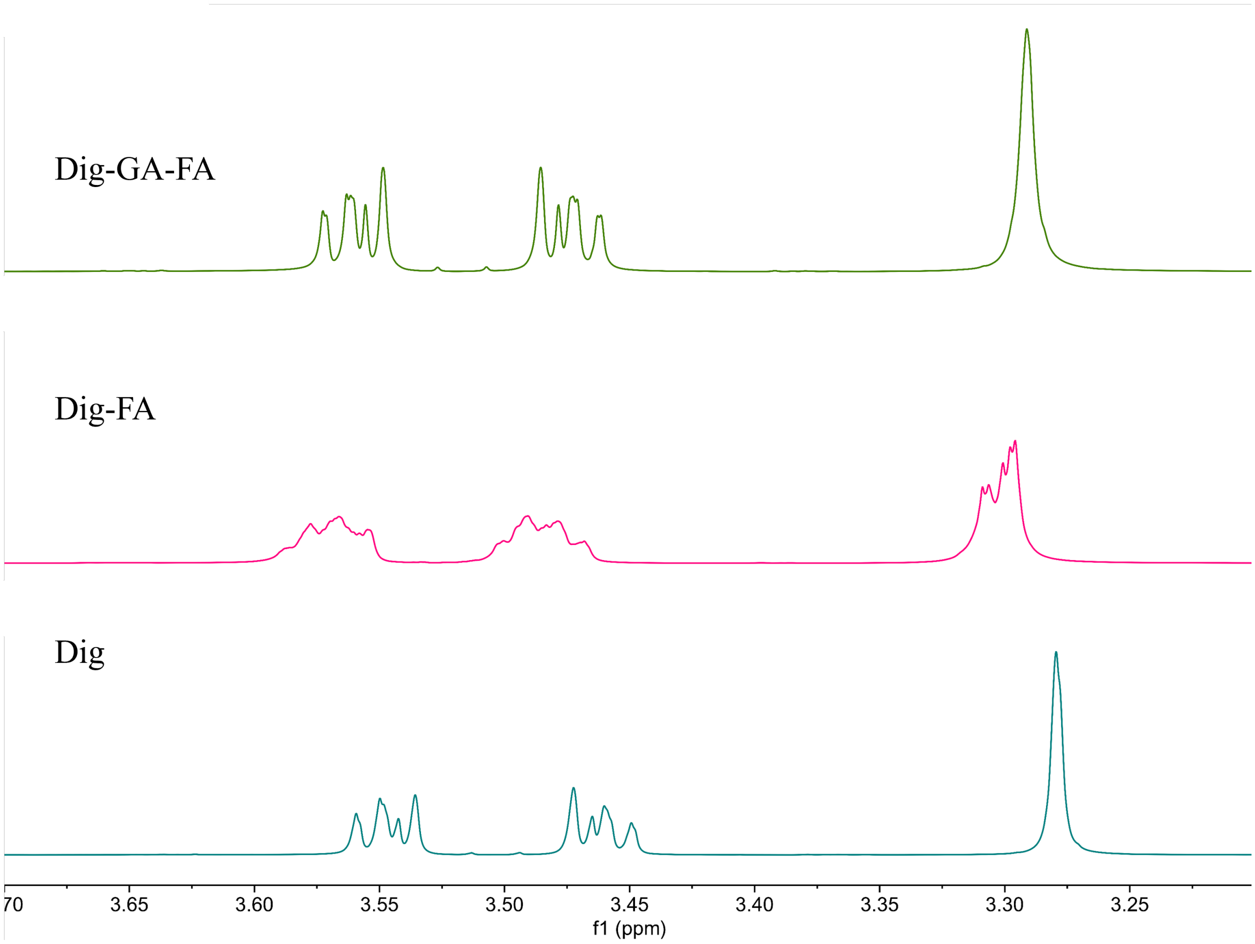

Figure S7: NMR spectra of Diglyme, FA dispersed into Diglyme and GA-FA mixture dispersed into Diglyme and centered onto Diglyme methylene and methyl chemical shift.

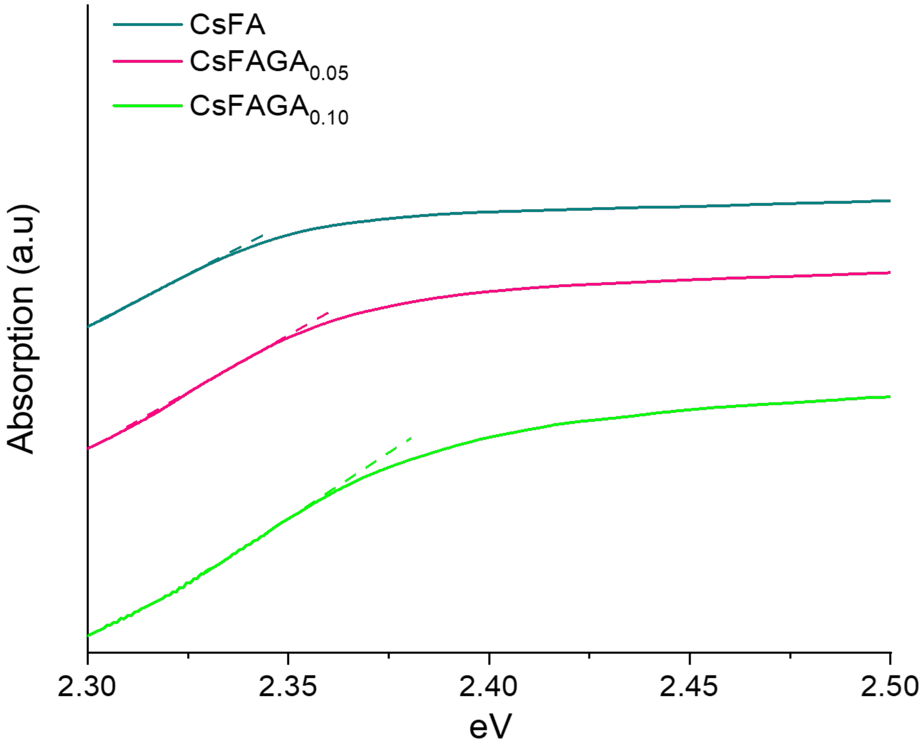

Figure S8: Evolution of the Urbach Energy calculated for pre-synthesized GA-doped triple cation PQDs. The Urbach Energy of CsFA is 69.8 meV, of CsFAGA$_{0.05}$ is 61.9 meV and 55.6 meV for CsFAGA$_{0.1}$, which is indicative of reduced defect trap state in the shallow level of the valence and conductance band.

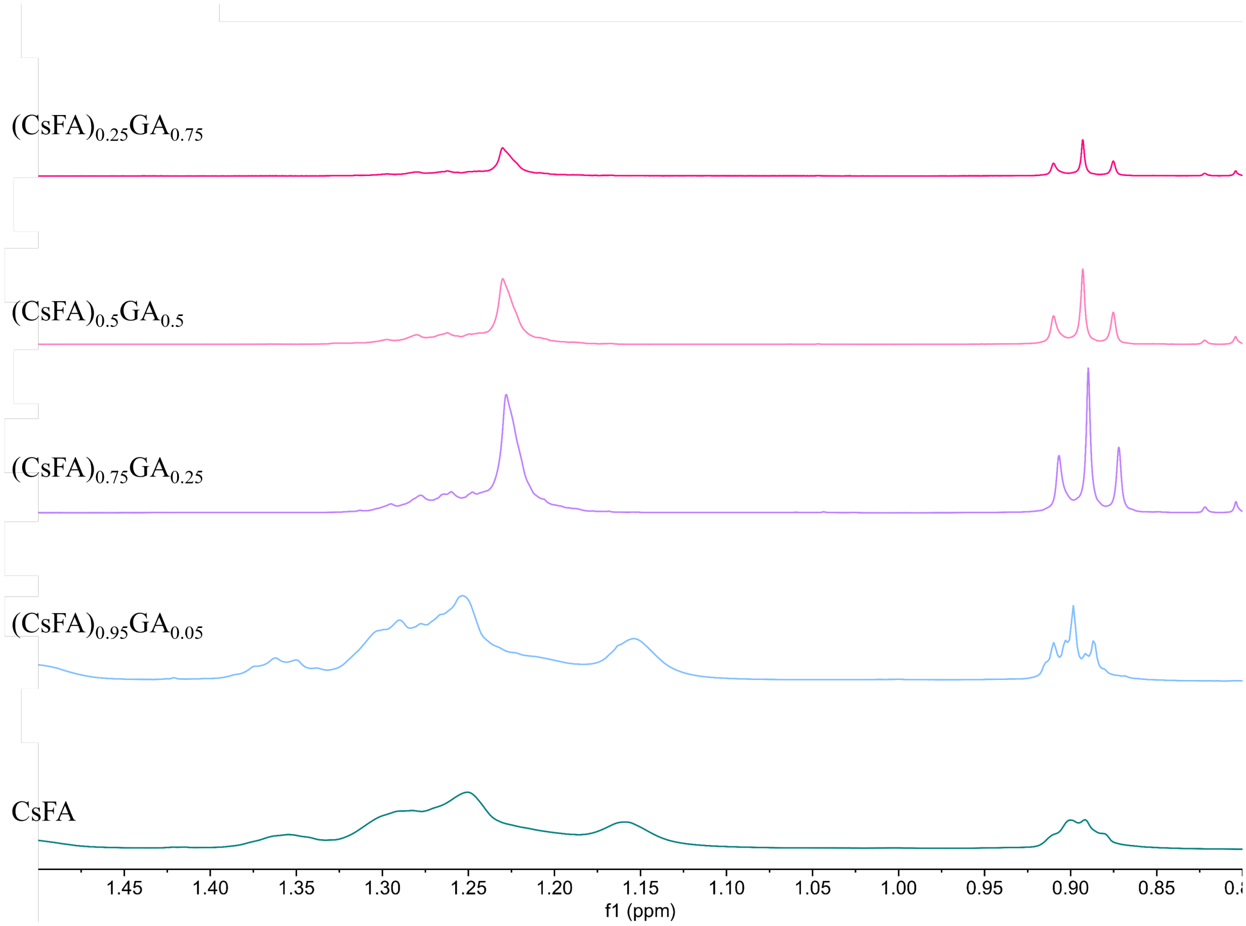

Figure S9: NMR analysis of all PQDs dispersed in toluene-d_8 for NMR characterization and the signal is centered on the 0.8 to 1.5 ppm region of PQDs surface ligand.

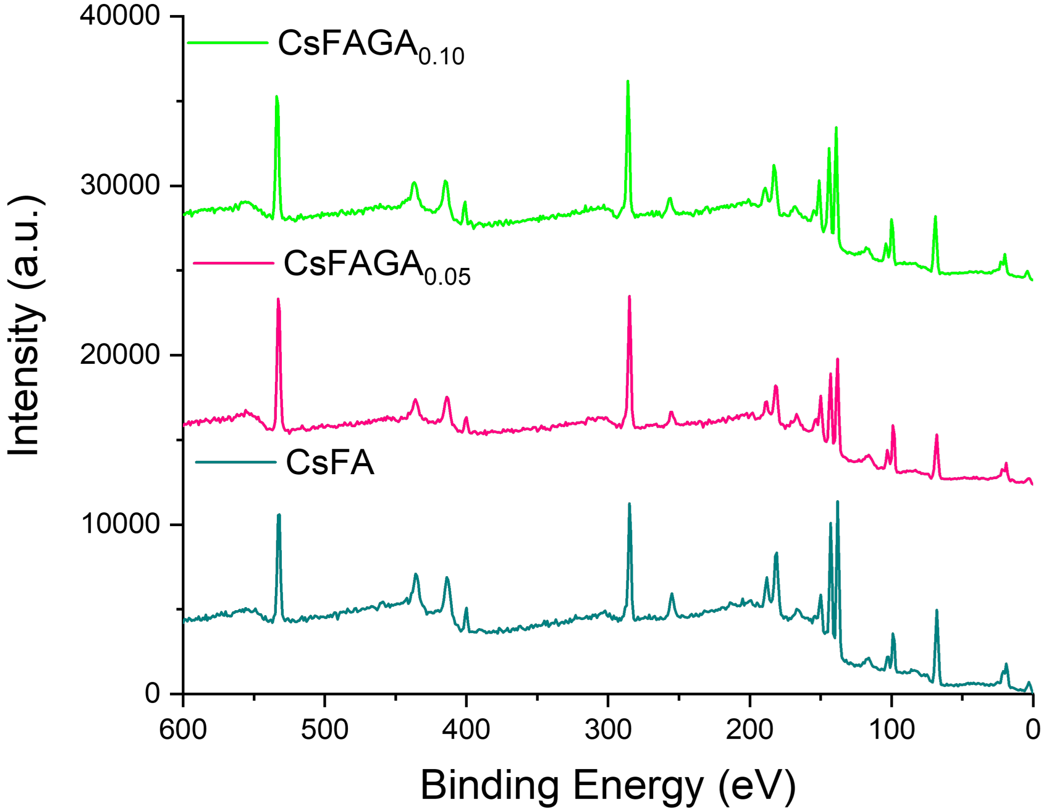

Figure S10. XPS spectra for pristine and GA-doped PQDs.

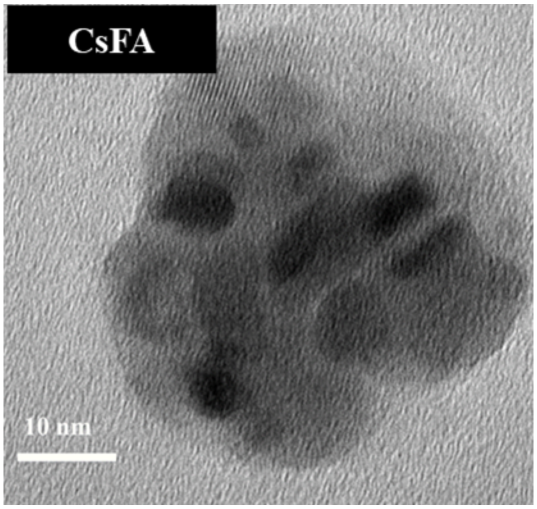

Figure S11. TEM observation of CsFA PQDs.

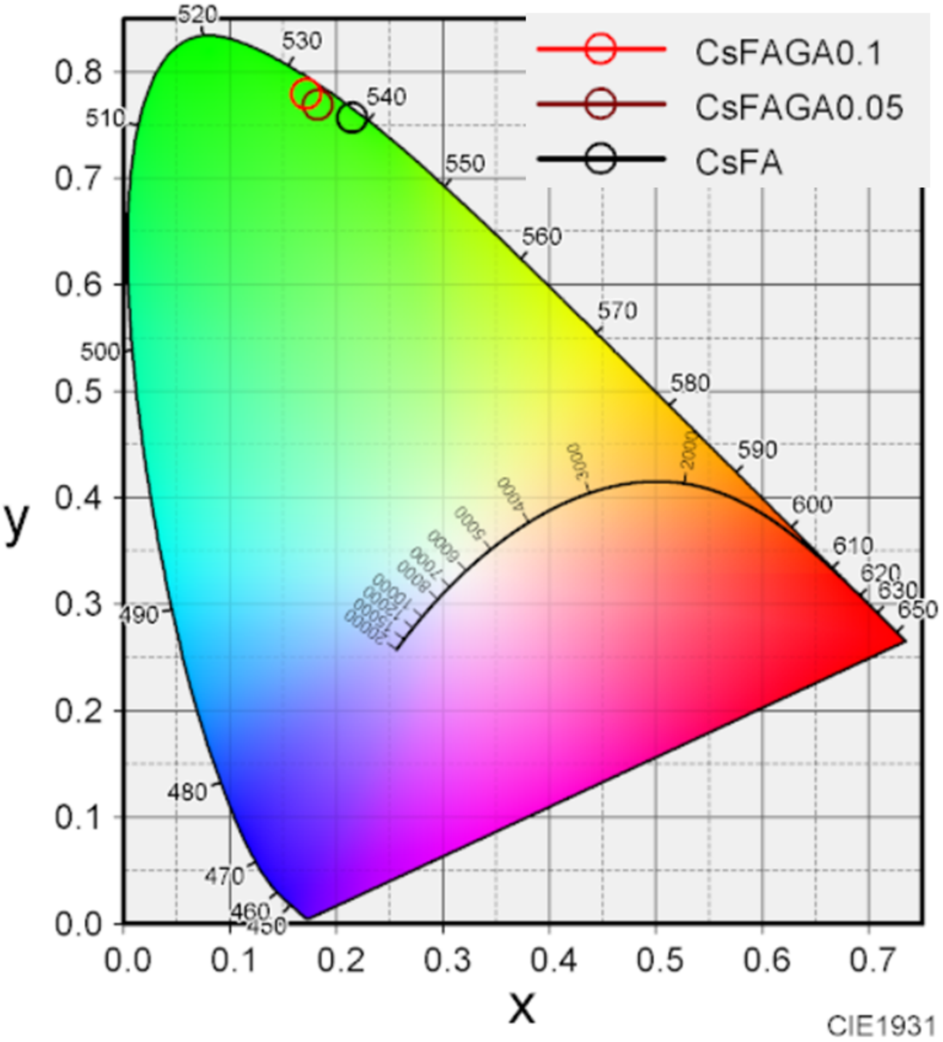

Figure S12. Evolution of the EL coordinate at the peak area according to the increase of GA ratio inside the PQDs.

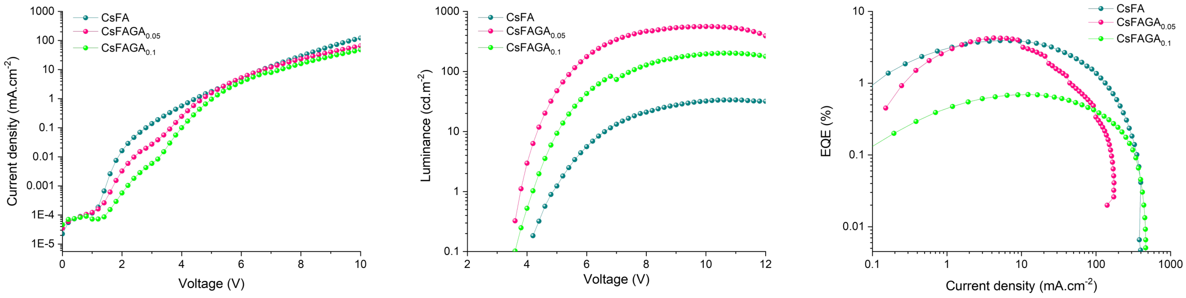

Figure S13. Preliminaries performances of LEDs device constructed with CsFA and CsFAGA PQDs using Poly-TPD as HTL.

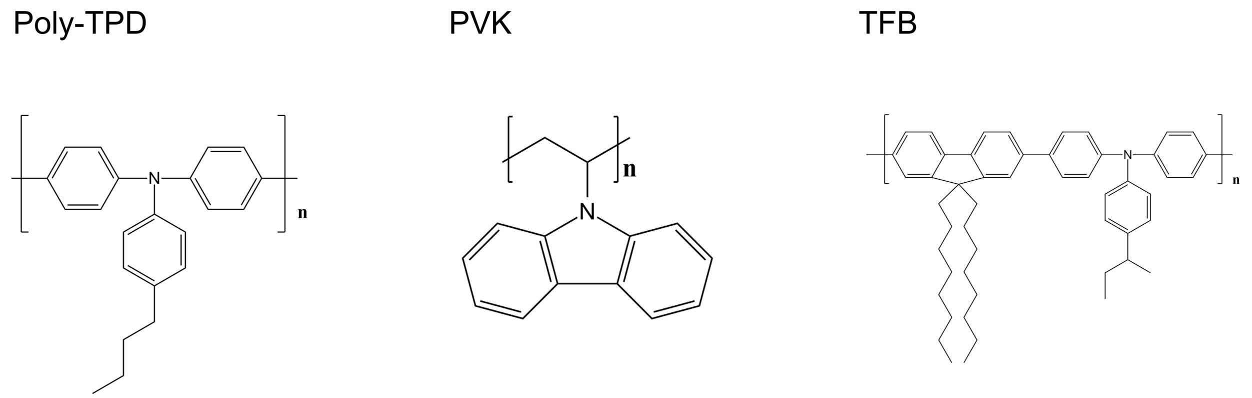
Poly-TPD

PVK

TFB

Figure S14. Chemical structure of Poly-TPD, PVK and TFB hole-transport layer.

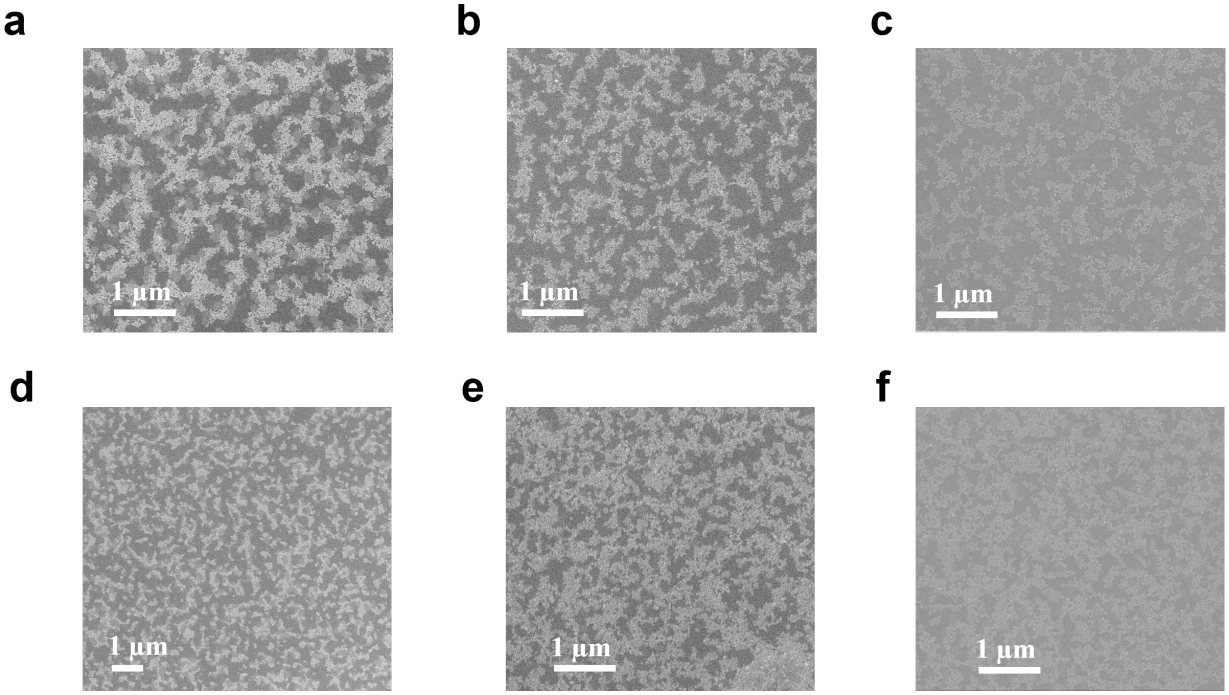

Figure S15. SEM picture of CsFA PQDs deposited on a) Poly-TPD, b) PVK and c) TFB hole-transport layer. SEM picture of CsFAGA$_{0.05}$ PQDs deposited on d) Poly-TPD, e) PVK and f) TFB hole-transport layer.

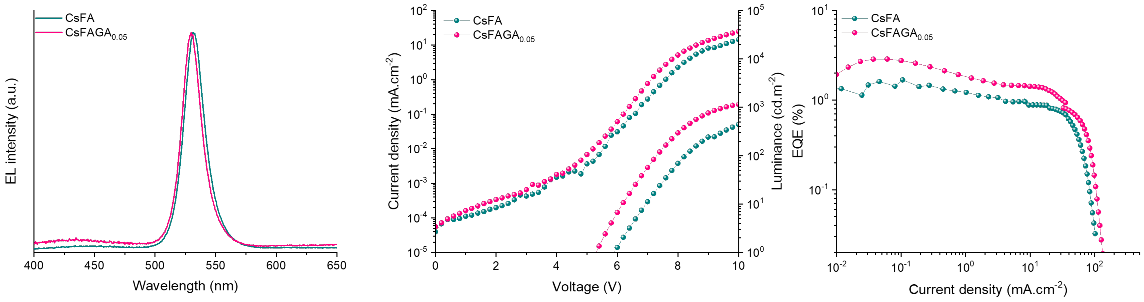

Figure S16. PVK-HTL fabricated LEDs devices performances while comparing CsFA and CsFAGA$_{0.05}$ PQDs active layer.

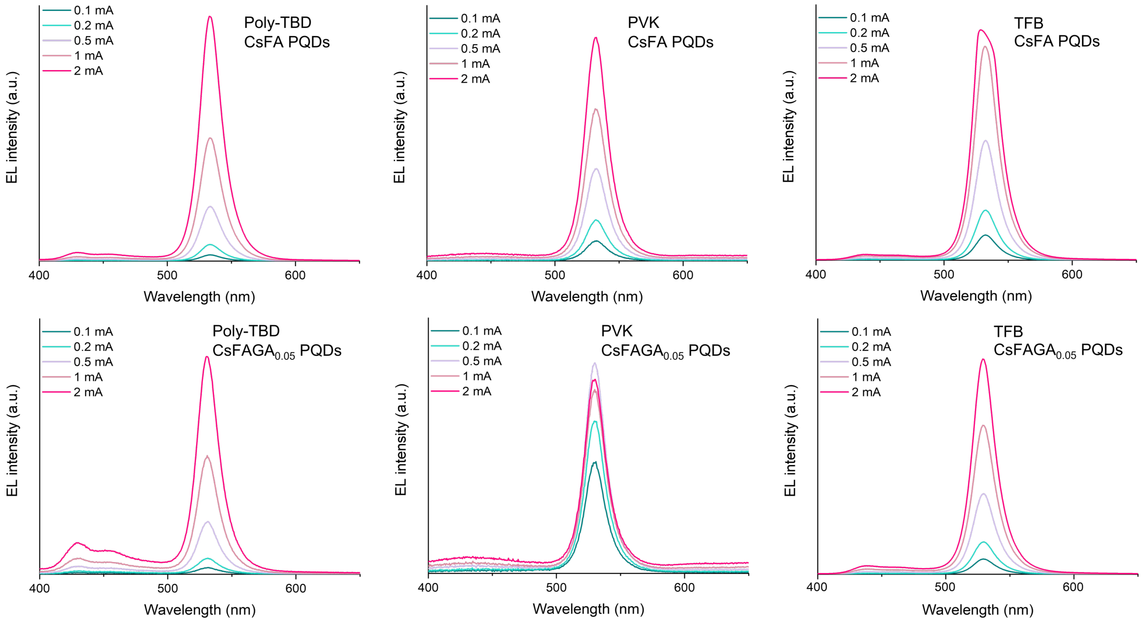

Figure S17. Evolution of the EL spectra while increasing the current intensity and modifying the HTL of the fabricated LEDs devices.